doi:10.2533/chimia.2024.862 Chimia 78 (2024) 862–868

The First Decade of Colloidal Lead Halide Perovskite Quantum Dots (in our Laboratory)

Dmitry N. Dirin and Maksym V. Kovalenko*

Abstract: Ten years after the discovery of colloidal lead halide perovskite nanocrystals (LHP NCs), the field has witnessed substantial progress in synthetic methods, understanding of their surface chemistry and unique optical properties, precise control over NC size, shape, and composition. Ligand engineering, particularly with cationic and zwitterionic head groups, massively enhanced NC stability, compatibility with organic solvents, and photoluminescence efficiency. These breakthroughs allowed for the self-assembly of monodisperse NCs into complex long-range ordered superlattices and enabled the exploration of collective optical phenomena, such as superfluorescence. The development of low-cost scalable approaches like microfluidic systems and mechanochemical synthesis paved the way for the commercialization of LHP NCs, particularly for the down-conversion films in blue-backlit LCDs and as thermally-efficient color converters in pixelated displays. This review aims to trace the journey of these advancements, focusing on contributions from Switzerland, and outline future directions in this rapidly evolving field, such as quantum light sources, photocatalysis, *etc.*

Keywords: Colloids · Lead halide perovskite · Nanocrystals · Photoluminescence

Maksym V. Kovalenko obtained an MS in Chemistry (2004) from Chernivtsi National University (Ukraine) and a PhD (2007) from JKU Linz (Austria). After postdoctoral training (2008–2011, at the University of Chicago, USA), he moved to Switzerland, and is now a full professor at ETH Zürich (Institute for Inorganic Chemistry) and Empa. His research encompasses bulk semiconductors for hard radiation detection, synthesis, surface chemistry, spectroscopy and self-assembly of quantum dots, as well as novel materials for rechargeable batteries. He has co-authored over 400 articles and is listed as an inventor on 16 patents.

Dmitry N. Dirin obtained his PhD degree from Moscow State University in 2011. In 2013, he moved as a Marie-Curie postdoctoral fellow to ETH Zürich, now working as a scientist in the Functional Inorganic Materials group. His research interests include the synthesis and surface chemistry of colloidal nanocrystals.

1. Discovery of Lead Halide Perovskite Nanocrystals

The rapid rise of lead halide perovskites (LHPs) in photovoltaics began between 2009 and 2012, driven by seminal works of T. Miyasaka, H. Snaith, and M. Grätzel, which demonstrated LHPs potential as highly efficient light absorbers with clean electronic behavior.[1] Over the next three years, the efficiency of LHP-based solar cells increased at an unprecedented rate, capturing widespread attention in the scientific community. It became evident that LHPs represented a distinct class of semiconductors with remarkable properties motivating the synthetic efforts towards developing LHP colloidal nanocrystals (NCs); in particular, of the size comparable to the exciton dimensions or smaller – quantum dots (QDs). Colloidally stable, brightly emissive $CsPbX_3$ (X=Cl, Br, I) QD solutions were successfully obtained through the reaction of cesium salts and lead halides, solubilized with oleate and oleylammonium counterions (Fig. 1a).[2] The size of $CsPbX_3$ NCs was tuned within the 4–15 nm range by adjusting the reaction temperature. Besides quantum confinement, the energy bandgaps were tuned by producing mixed-halide LHPs – $CsPb(Cl/Br)_3$ and $CsPb(Br/I)_3$. Additionally, the halide content could be modified post-synthetically, readily at room temperature, by adding an excess of the corresponding halide.[6] Later on, the group further expanded the compositional diversity of LHP NCs to hybrid organic-inorganic $APbX_3$ (A= Cs, methylammonium (MA), formamidinium (FA), or aziridinium (AZ)).[7]

The facile synthesis, compositional tunability, and bright photoluminescence (PL) of the obtained NCs sparked significant attention and marked a milestone in colloidal QD research. The facile anionic exchange was new to this field, as well as unusual structural softness and high entropy. LHP NCs possess not only a dynamic structure allowing substantial compositional changes (Fig. 1b),[3,8] but also dynamic surface chemistry (Fig. 1c),[4] maintaining colloidal stability and avoiding deep trap states despite numerous structural defects. What made LHP NCs most intriguing was the combination of bandgap tunability with high PL quantum yield (PL QY). The latter typically requires epitaxial overcoating with wide-bandgap shells for electronic passivation of more conventional QD materials (chalcogenides, pnictides). A similar behavior was observed in bulk $MAPbI_3$, where its ability to maintain a low number of trap states despite a high defect density was attributed to defect tolerance (Fig. 1d).[5] In LHPs, defect tolerance refers to their unique electronic structure, where defects like vacancies or interstitial atoms do not create charge-trapping states within the bandgap. This is due to the valence band comprising antibonding orbitals between lead and halide ions, preventing common defects such as halide vacancies from forming mid-gap states. Instead, defects typically create resonances within

*Correspondence: Prof. Dr. M. V. Kovalenko, E-mail: mvkovalenko@ethz.ch
Department of Chemistry and Applied Biosciences, ETH Zurich, Vladimir-Prelog-Weg 1, CH-8093 Zürich; Empa – Swiss Federal Laboratories for Materials Science and Technology Laboratory for thin films and photovoltaics Ueberlandstrasse 129, CH-8600 Dübendorf

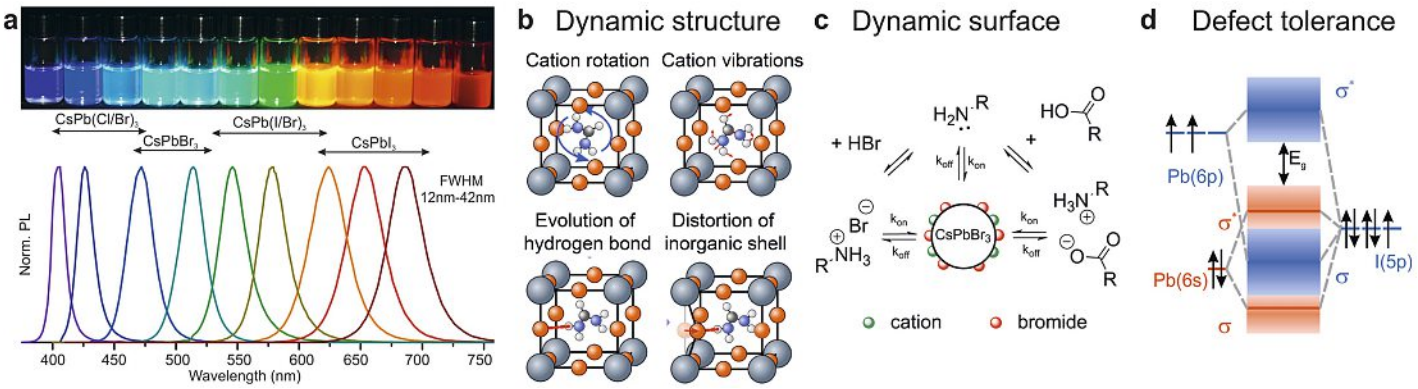

Fig. 1. The first examples of $CsPbX_3$ NCs, including their facile compositional and size-tunability of PL peak wavelength (a). The $APbX_3$ compounds are characterized by complex lattice (b) and surface (c) dynamics, and unusual electronic structure (d) tolerant to common structural defects. Adapted with permission: (a) from ref. [2], (b) from ref. [3], (e) from ref. [4], (f) from ref. [5].

the conduction or valence bands. The tolerance of optical properties to structural defects, combined with low formation energy and dynamic surface chemistry, opens up diverse synthetic possibilities. These factors have shaped the group's three key research areas for LHP NCs in the coming years. The following chapters explore how these preliminary observations led to: (i) exploration of synthetic possibilities (and challenges) enabled by structural dynamics and low formation energy; (ii) advancements in surface chemistry through a diverse library of ligands with tailored binding groups and functionalities; and (iii) a deeper understanding of LHP NCs' optical properties.

2. Diverse Synthetic Approaches to LHP NCs

The first synthetic approaches to LHP NCs employed either hot-injection (HI) or antisolvent-induced ligand-assisted reprecipitation (LARP) reactions (Fig. 2a). LARP had initially gained popularity for its simplicity, scalability, and low-temperature process but faced challenges in controlling NC size and shape, resulting in broader size distributions. Additionally, LARP-produced NCs were less stable due to insufficient surface passivation and residual impurities from polar solvents. In contrast, the HI method offered superior control over NC quality, yielding improved optical properties and long-term stability.

Motivated by the challenges of both methods – especially the rapid NC formation kinetics – the group engaged in collaborative efforts on microfluidic synthesis for LHP NCs (Fig. 2b).[9] Unlike traditional batch reactions, which struggle to adequately control fast nucleation and growth, microfluidic systems afford millisecond rates for reagent mixing. Each droplet can be adjusted to have different precursor ratios or concentrations. Combined with in-line PL and absorption measurements, microfluidics affords rapid mapping of the parametric space. Mixed $CsPb(Br,I)_3$ NCs were found not to form directly, but through the transient monohalide NCs exchanging and homogenizing their content at a later stage;[9a] $FAPbBr_3$ grew *via* intermediate nanoplatelets, unlike $FAPbI_3$, which directly formed cubic near-infrared-emitting NCs.[9b]

The facile formability of LHP NCs was harnessed for their synthesis in confined spaces of mesoporous silica templates (Fig. 2c).[5] Although such templates have already been used for conventional QDs like CdSe and CdS, achieving efficient PL in those systems is challenging due to the need for proper surface passivation to prevent deep trap states. In contrast, LHPs' defect tolerance bypassed this limitation, allowing bright PL without NC surface passivation. We thus were motivated to explore the heterogeneous nucleation for LHP NCs further. LHPs of various compositions can be heterogeneously grown on salt carriers while exhibiting bright, narrow-band PL despite the broad NC size distributions (Fig. 2d).[10]

The soft nature of LHPs, ease of crystallization, defect tolerance, and bright PL, even in the weak confinement regime, suggested the viability of top-down approaches such as mechanochemistry (Fig. 2e),[11] which is of particular practical value. The method involves mechanically grinding bulk $APbX_3$ or AX + PbX_2 mixtures in a solvent and ligands. Scalable quantities of $FAPbBr_3$ and $CsPbBr_3$ NCs were produced, albeit with a broader size distribution than those from HI. They nevertheless still exhibit PL spectra (22-30 nm) and high PL quantum yields (QYs) of up to 80%.

Most studies on colloidal LHP NCs have focused on larger sizes (≥8 nm) due to their soft, ionic structure, contrasting with the covalent and rigid nature of conventional QDs like CdSe or InP. This structural softness and fast ionic coprecipitation kinetics complicate the precise size control needed for small LHP QDs, limiting the exploration in strong quantum confinement regime. Achieving monodispersity and shape uniformity in the sub-10-nm range requires a scalable synthesis method for slow, controlled NC growth. We hypothesized that achieving a mutual chemical equilibrium between the precursor, monomer, and NC nuclei, mediated by a weakly binding complexing agent, could allow for controlled growth without interference from strong-binding ligands. Trioctylphosphine oxide fulfilled this role by solubilizing the $PbBr_2$ precursor, binding to $Cs[PbBr_3]$ monomers, and weakly coordinating to the NC surface. This enabled room-temperature synthesis, with 3–13 nm large monodisperse NC formation occurring over 30 minutes (Fig. 2f).[12] This method also enabled the first synthesis of monodisperse $FAPbBr_3$ and $MAPbBr_3$ QDs with tunable sizes down to 4-5 nm. The slow growth of NCs in the presence of only a weakly binding ligand allowed the introduction of a stronger one – lecithin – at the end of the synthesis, effectively separating the growth and passivation steps.

3. Surface Chemistry of LHP NCs

Dynamic surfaces and defect tolerance in LHP NCs provide a versatile platform for ligand engineering. Recent advancements in ligand design for LHP NCs are organized here by separately considering the head group and the tail (Fig. 3a).

The head group primarily determines surface passivation efficiency and NC stability against polar moieties. Early studies with oleylammonium and oleate ligands revealed two kinds of instability: their simultaneous desorption and the deprotonation of oleylammonium, which led to the loss of the ligand shell (Fig. 1c).[4] This resulted in poor surface passivation, weak PL, and limited colloidal stability and structural integrity. Two strategies were developed to address stability issues (Fig. 3b). The first involves using cationic ligands that resist deprotonation, such as quaternary dimethyldidodecylammonium bromide (DDAB)[14] or ole-

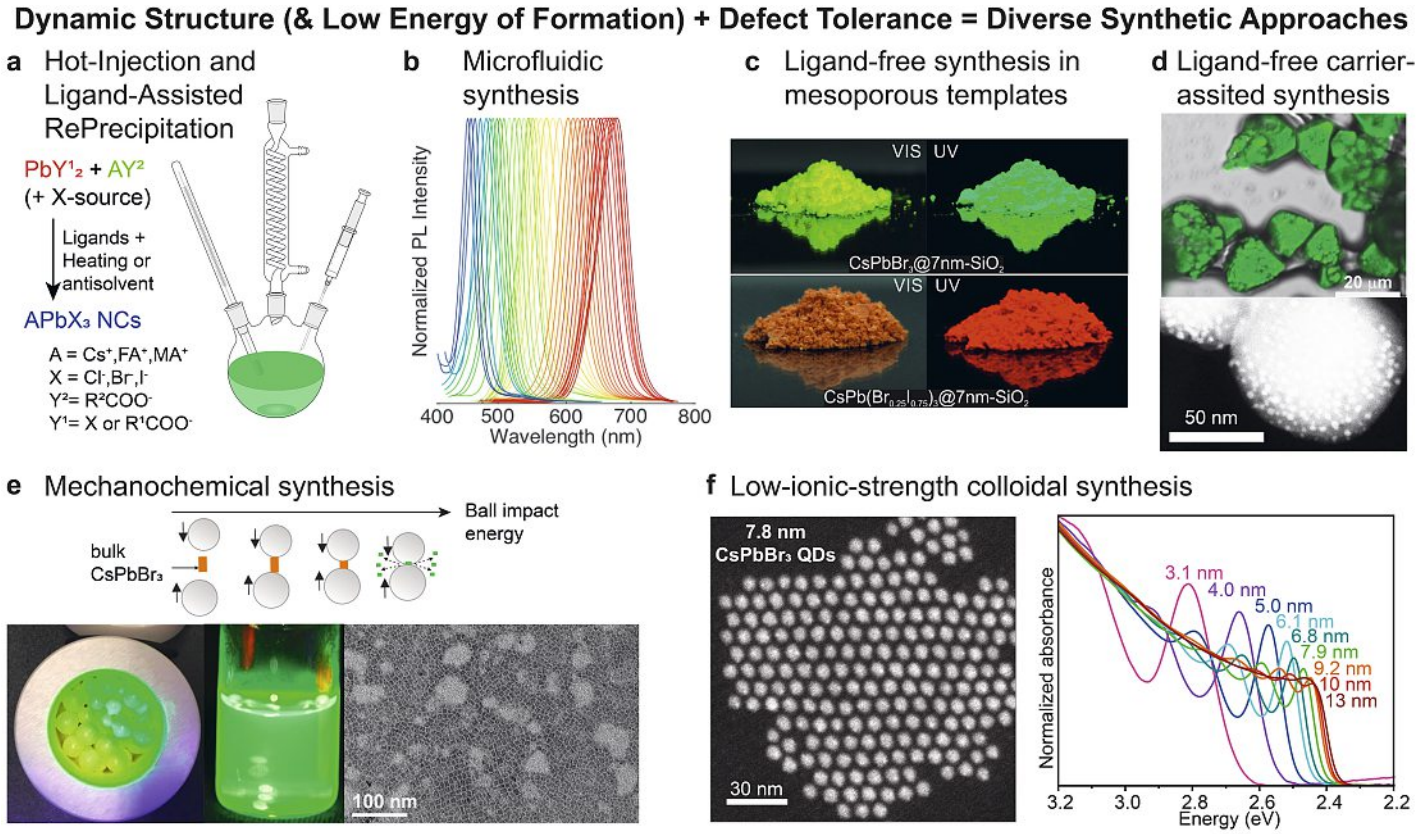

Fig. 2. Diversity of synthetic approaches to LHP NCs. (a) Schematic of HI and LARP methods using metal halide or carboxylate precursors. (b) PL spectra of $CsPbX_3$ NCs obtained in microfluidic synthesis. (c) Photographs of the $APbX_3$ NCs grown in the pores of mesoporous silica. (d) Confocal microscopy image of NaBr microcarriers decorated with $FAPbBr_3$ NCs and HAADF-STEM image of the same sample. (e) Schematics of the ball-milling synthesis, photographs showing corresponding colloid of $CsPbBr_3$ NCs and TEM image of the resulting NCs. (f) STEM image and absorption spectra of $CsPbBr_3$ NCs obtained by the low-ionic strength synthesis. Adapted with permission: (b) from ref. [9a], (c) from ref. [5], (d) from ref. [10], (e) from ref. [11], (f) from ref. [12].

ylguanidinium bromide with high pK_a.[19] DDAB-capped $CsPbBr_3$ NCs demonstrated superior stability, maintaining a high PL QY of up to 95–98% even after multiple purification cycles (Fig. 3c).[14] High PL QY is attributed to the halide-rich environment favored by cationic ligands, restoring the damaged PbX_6 octahedra.[14,20] Full restoration can be achieved through post-synthetic DDAB/$PbBr_2$ treatment and in a direct synthesis with DDAB.[21] This approach proved effective for fabricating LHP NC-based LEDs, where shorter ligand chains and the absence of inactive additives enable closer packing and improved charge transport.[21,22]

Zwitterionic ligands represent the second strategy for enhancing the stability of LHP NCs (Fig. 3b). Unlike traditional ammonium and carboxylate ligands, zwitterionic ligands offer two key advantages: they avoid mutual or external neutralization by virtue of the Brønsted acid-base interactions and benefit from the bidentate binding.[23] The first zwitterionic ligands introduced for LHP NCs featured head groups like sulfobetaine, phosphocholine, and γ-amino acid, all with quaternary ammonium cationic functionality.[23] A significant improvement was attained by shifting to synthetic phosphoethanolamines, owing to the better fitness of the primary ammonium group to the A-site pocket on the NC surface.[13] These NCs showed remarkable PL QYs (>96%) in both solution and solid states, with minimal PL intermittency and a high ON fraction (94%) for single-particle emission. Notably, these ligands can be applied through post-synthetic exchange and direct synthesis, offering broad potential for various applications. Aside from the anionic and cationic groups of zwitterionic ligands, the bridge length between them can also be adjusted to match the LHP lattice.[23]

Zwitterionic ligands changed the landscape for LHP NCs stability, purification, and solvent compatibility. Sulfobetaine-, phosphocholine-, and phosphoethanolamine-based ligands render LHP NCs sufficiently stable to withstand multiple cycles of precipitation with polar solvents for purification or size selection (Fig. 3d),[15] and yield highly dilute (4 ng/ml) yet stable solutions.[23,24]

To compare the stabilization effects of various ligands, a systematic study was conducted on anion exchange rates in $CsPbX_3$ NCs (Fig. 3e).[16] The results indicated that anion exchange is facilitated by surface capping ligands, which form a counter pair with desorbed anions and diffuse to other NC surfaces to initiate the exchange. Zwitterionic ligands significantly slow anion exchange compared to the alkylammonium/oleate pair, with lecithin-capped NCs showing the highest stability among tested. To further explore lecithin's binding and its effect on the $CsPbX_3$ (X = Cl or Br) core-to-surface structure, solid-state NMR with dynamic nuclear polarization (DNP) and atomistic molecular dynamics (MD) simulations were employed.[17] These analyses confirmed the direct binding of phosphate groups ($-PO_4^-$) to subsurface Pb atoms and revealed the presence of $-N(CH_3)_3^+$ groups near the surface ^{133}Cs atoms. Based on these findings, a model is proposed where the $CsPbX_3$ NC surface is terminated by a CsX layer, with partial substitution of Cs^+ and X^- ions by ligand headgroups $-N(CH_3)_3^+$ and $-PO_4^-$ (Fig. 3f).

These findings indicate significant variation in ligand binding dynamics to the NC surface among common ligands used for LHP NCs (Fig. 3g). At one end, the alkylammonium/oleate pair exhibits highly dynamic binding, while phosphocholine – and likely phosphoethanolamine – shows more static binding. These differences underscore the importance of selecting appropriate ligands to optimize NC stability for specific applications.

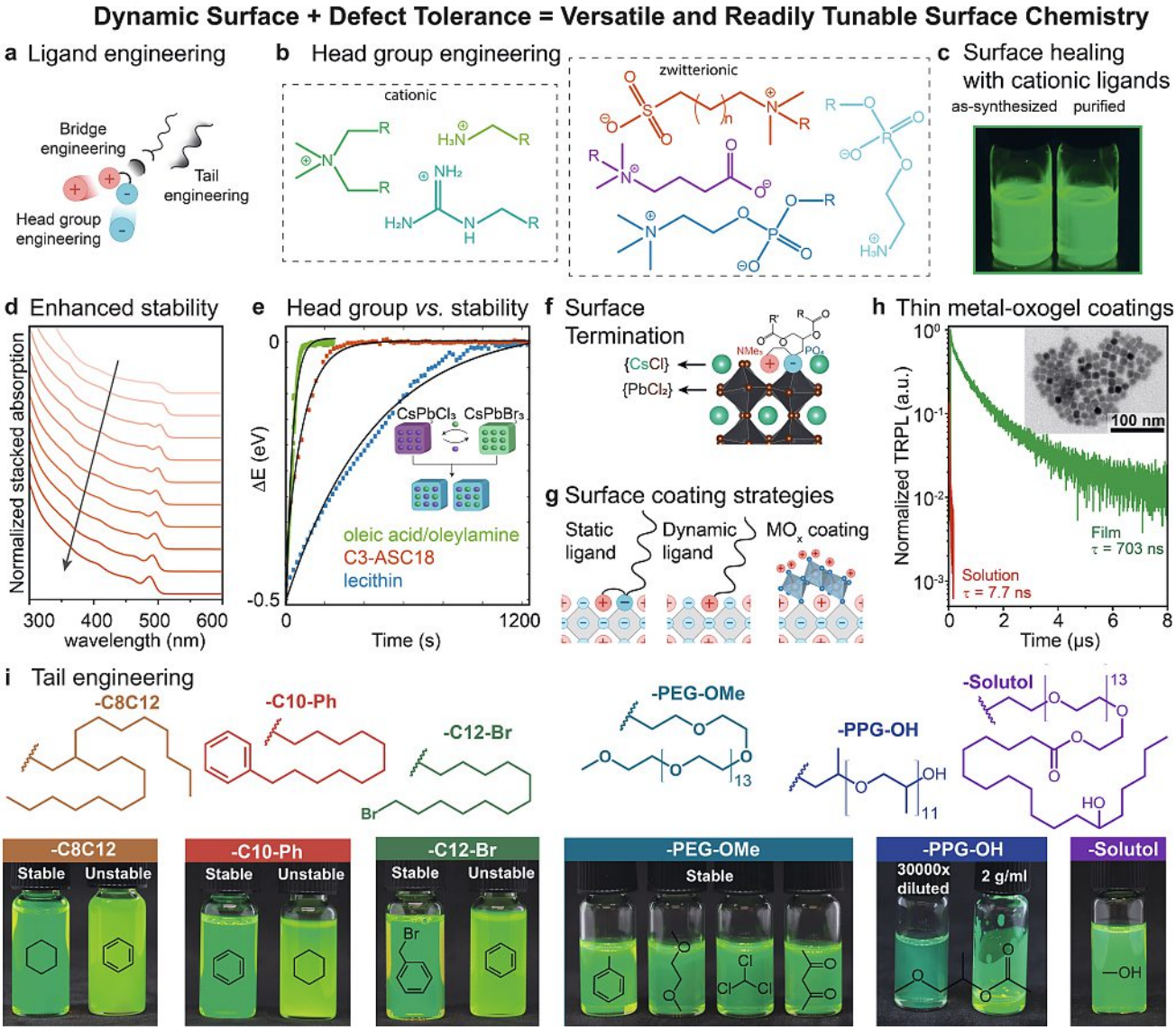

Fig. 3. Versatile surface chemistry of LHP NCs. (a) Schematic of ligand engineering. (b) Library of ligand head groups applied to LHP NCs. (c) Photographs of as-synthesized and purified DDAB-coated $CsPbBr_3$ NCs under UV light. (d) size selective precipitation of $CsPbBr_3$ NCs; the arrow indicates a progressively increased amount of added polar antisolvent. (e) The ligand effect on the stability of $CsPbBr_3$ NCs towards anion exchange is illustrated as the PL peak position difference from the one stabilized at the end. (f) Lecithin binding to the surface of $CsPbCl_3$ NCs as revealed by NMR spectroscopy. (g) Three types of LHP NCs surface coating. (h) TRPL of alumina-gel-coated $CsPbBr_3$ NCs in solution and compact film, illustrating coupling of NCs in the latter. Adapted with permission: (a, i) from ref. [13], (c) from ref. [14], (d) from ref. [15], (e) from ref. [16], (f) from ref. [17], (h) from ref. [18].

Beyond organic-ligand coating, we explored a distinct passivation strategy using ultra-thin metal oxide gel coatings.[18] Sub-nanometer (<1 nm) coatings were applied to 5–14 nm large $CsPbX_3$ NCs *via* non-hydrolytic sol-gel reactions, enabling dispersibility and stability in short-chain alcohols while maintaining high PL QY of 70–90%. The thin coatings, with their high dielectric constant, enabled electronic and excitonic coupling in compact NC films, resulting in PL lifetimes extended to 400–700 ns – two orders of magnitude longer than those of NCs with organic ligands or the same NCs dispersed in solution (Fig. 3h). These properties make the coated NCs ideal for applications requiring efficient charge carrier delocalization or extraction.

While the ligand head group primarily governs NC integrity and chemical stability against polar environment, the ligand tail dictates which solvents can dissolve NCs at high concentrations and which act as antisolvents. Thus, natural lecithin ligands – with their branched chains and polydispersity that enhance particle-particle repulsion – enable highly concentrated solutions (over 400 mg/ml).[24] High concentration allowed a single-step deposition of thick (up to 1.5 μm) NC film with maintained optical clarity and bright fluorescence. More recently, we developed a library of ligands with tailored tail functionalities enabling solvent compatibility across a broad polarity range, from hydrocarbons to alcohols (Fig. 3i).[13]

4. Superlattices of LHP NCs

Advances in controlling the synthesis and surface chemistry of LHP NCs have enabled solutions of highly monodisperse NCs, with a standard size deviation below 5%, a key requirement for their self-assembly into long-range, single-component superlattices (Fig. 4a). Furthermore, the cuboidal shape of $CsPbBr_3$ NCs allows for facile ligand-deformability at the vertices and edges, enabling denser packing than spherical NCs. This has proven to be the key to obtaining binary and ternary superlattices that differ significantly from all-sphere assemblies.[25]

Three of the structures obtained in small cube-large sphere and small cube-large truncated cube mixtures are exclusive to the use

of cubes as the smaller component: AB_2, b-ABO_6, and b-ABO_3 (Fig. 4b).[25,27,28] These structures become accessible due to much higher packing densities when using cubes instead of spheres. Similar structures have been achieved using only LHP NCs of varying sizes.[29] Two substrate-free methods for superlattice formation were demonstrated: oil-in-oil templated assembly for binary supraparticles and self-assembly at the liquid-air interface for extended thin films (Fig. 4c).[27,30]

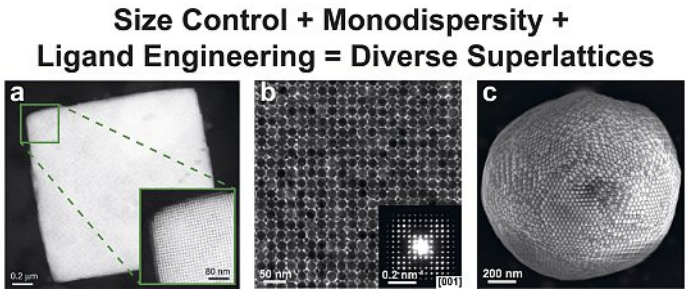

Fig. 4. (a) HAADF–STEM image of $CsPbBr_3$ NC superlattice; inset shows a magnified view of the boxed area, showing the individual NCs.(b) TEM image of ABO_3-type superlattice of $CsPbBr_3$ and Fe_3O_4 NCs, along with the corresponding small-angle electron diffraction pattern (inset). (c) SEM images of supraparticles with CaC_2-like structure assembled from $CsPbBr_3$ and $NaGdF_4$ NCs. Reproduced with permission: (a) from ref. [26], (b) from ref. [25], (c) from ref. [27].

5. LHP NCs as Classical and Quantum Light Sources

LHP NCs achieve near-unity PL QYs at room temperature without the need for a passivating inorganic shell, setting LHP NCs apart from earlier generations of colloidal QDs. Moreover, LHP NCs maintain bright PL even for larger sizes exceeding this material's exciton Bohr diameter (6-7 nm). In such a weak-confinement regime, inhomogeneous broadening related to NC size and shape distribution is much reduced, yielding narrow-band ensemble emission with typical line widths of 70–90 meV (*ca.* 20 nm) for large (>8 nm) $CsPbBr_3$ NCs.[31] These narrow emission lines translate into a high color purity. Importantly, LHP NCs offer superior color purity in green region, which, as the central wavelength for human eye sensitivity, is the most critical component for achieving a wide color gamut (Fig. 5a). Aside from a costly combination of green CdSe with red InP QDs, LHP NCs are the only RoHS-compliant QDs with a color gamut approaching the Rec.2020 color space.[32] This combination of superior optical properties, together with their accessibility *via* low-cost and scalable microfluidic and mechanochemical synthetic approaches, makes LHP NCs appealing candidates for display applications.

LHP NCs are already produced by Avantama AG on an industrial scale as luminophores for down-conversion films combined with blue or magenta LED backlighting – so-called QD enchancement films or QDEFs.[33] By combining the green LHP QD film with a magenta backlight (blue LED + KSF phosphor) the QDEF-based display reaches > 90 % Rec.2020 color space coverage while surpassing the required 1000 hours stability threshold in the common accelerated temperature, humidity and light flux stability tests.[34] In QDEFs, the generated three-component light passes through color filters, transmitting only the desired light component (Fig. 5b). While this represents the state-of-the-art technology, it has limited energy efficiency, as a substantial portion of the generated three-component light must be filtered out by color filters to display pure colors. The true potential of LHP NCs in display technologies may be realized in the next-generation displays, where NCs are used not in combination with, but instead of, color filters (Fig. 5c).[35] In this scheme, green and red light components are produced by the full color conversion of blue light into green and red using thick QD layers deposited directly onto the individual blue LED pixels. The main advantage of using QDs as color converters is an improvement of up to 50% in energy efficiency compared to current LCD (and QDEF) displays.[36] This technology is best combined with small-pixel OLEDs (QD-OLED) and microLEDs (QD-microLED). Combining QDs' pure colors with OLEDs' superior contrast and wide viewing angles enhances the viewing experience. QD-microLED, on the other hand, fulfills another display niche by combining long lifetimes with nanosecond-fast response times, which are critical for 3D/AR/VR displays.[37]

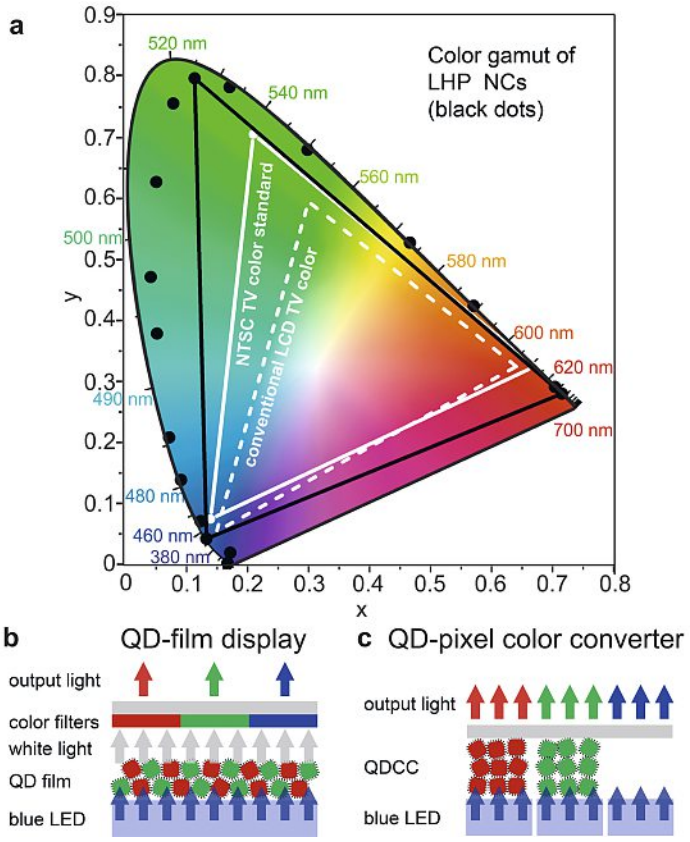

Fig. 5. LHP NCs are efficient classical light sources with high color purity for display applications. (a) The color gamut of LHP NCs (reproduced with permission from ref. [2]). The operational principle of QDEF (b) and pixelated QD color converter (c) displays.

One major requirement for using QDs as color converters is the ability to deposit them using photolithography or printing – common methods for producing small, pixelated structures. High-quality patterned LHP QD films, made using inkjet printing (200-μm pixel pitch), photolithography (45-μm pixel pitch), and electrohydrodynamic printing (12.5-μm pixel pitch), have been successfully demonstrated.[38] Another requirement is that QD color conversion layers must absorb 99% of the incoming blue light, setting demanding criteria for absorption efficiency given the technologically limited layer thickness. In this regard, LHP QDs are particularly promising compared to InP QDs because they have high absorption coefficients, do not require thick inorganic shells, and thus utilize film space more efficiently, leading to high optical densities (up to 2-3) in thin (3 to 4.5 μm) films.[38]

In addition to their outstanding optical properties as classical light sources, LHP NCs exhibit a highly unusual electronic structure, which turned out to be a key factor in unlocking quantum many-body phenomena both in individual NCs and in NC superlattices. The fine structure analysis of low-temperature single-NC fluorescence spectra of $CsPbX_3$ NCs revealed that, unlike for organic semiconductors and any other known inorganic semiconductor, the emission in $CsPbX_3$ NCs is dominated by bright

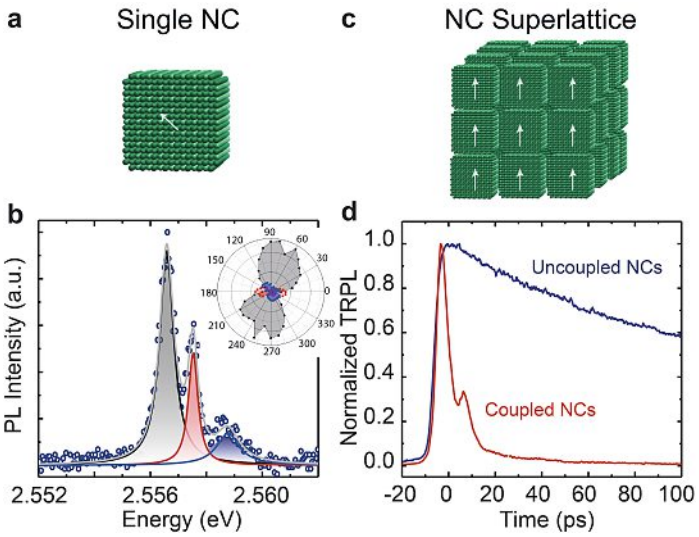

Fig. 6. Schematic (a) and low-temperature PL spectrum (b) of a single $CsPbBr_3$ NC exhibiting bright triplet exciton states. The inset shows the linear polarization of each of the spectral features. (c) Schematic of an NC superlattice and (d) time-resolved PL decay for uncoupled NCs (blue line) and coupled NCs (red line) in the superlattice. Adapted with permission: (a, c) from ref. [39], (b) from ref. [40], (d) from ref. [26].

triplet excitons (Fig. 6a,b).[40] The bright triplet character of the exciton with orthogonal dipole orientations exhibits an unusually high oscillator strength, yielding an ultrahigh radiative rate, 20 and 1000 times faster than in any other QD platform at room and cryogenic temperatures, respectively. Recently, the origin of this fast decay at cryogenic temperature was explained by the occurrence of single-photon superradiance (SPS).[41] In this case, the exciton wavefunction delocalizes over a region larger than the Bohr diameter. This enables all unit cells within the coherence volume to cooperatively respond to excitation, forming a giant transition dipole with enhanced oscillator strength. This collective behavior results in excitonic SPS with accelerated radiative decay, where the maximum rate enhancement scales with the number of unit cells participating in the exciton coherence volume. In 2024, we reported SPS in individual 30 nm $CsPbX_3$ NCs, achieving sub-100 picosecond radiative decay times, nearly matching the exciton coherence times (*ca.* 80 ps for large $CsPbBr_3$ NCs owing to reduced exciton-phonon coupling).[42] Size-, composition-, and temperature-dependent studies further confirmed the formation of giant transition dipoles. Unlike traditional methods that enhance PL brightness *via* photonic state engineering, this work utilized the collective behavior of weakly confined excitons.

The fast (down to *ca.* 100 ps) radiative recombination, on par with long exciton coherence times observed in LHP NCs, suggests the possibility of achieving collective optical phenomena in NC superlattices (Fig. 6c,d). In 2018, our colleagues from IBM Zürich reported superfluorescence in $CsPbBr_3$ NC superlattices. Superfluorescence occurs when several neighboring NCs synchronize their dipoles, forming a single giant dipole that produces short, intense bursts of light proportional to the square of the number of coupled emitters. The PL spectrum of these superlattices at cryogenic temperatures showed two distinct bands, with the redshifted band corresponding to coupled NCs. Importantly, time-resolved PL spectroscopy further revealed significantly faster radiative decay for this lower-energy band, with radiative lifetimes dropping to 20 ps under high excitation densities, suggesting the involvement of more than ten coupled NCs (Fig. 6d).

6. Outlook

Over the past ten years, the synthesis and understanding of LHP NCs have progressed at an extraordinary pace, enabling superior control over their quality, size, and composition. Ligand engineering, particularly with cationic and zwitterionic ligands, has dramatically improved the NC stability, enabling multiple purification cycles, size-selective precipitation, and long-term stability across a wide solvent-polarity range while maintaining near-unity PL QYs. These advancements have also enabled the self-assembly of monodisperse NCs into superlattices and a better understanding of their surface chemistry and optical properties. Nevertheless, these remarkable achievements brought a new set of challenges, some of which are highlighted below:

1) The controlled synthesis of anisotropic LHP NCs, such as nanorods and nanoplatelets, remains to be demonstrated. While the synthesis of $CsPbBr_3$ nanoplatelets has been known for several years, their stability is still suboptimal. Shape engineering will be pivotal for adjusting the exciton fine structure while maintaining fast radiative rates.
2) We anticipate that the slow, low-ionic strength reaction developed recently for LHP NCs[12] and phospholipid-capping[13] will be highly instrumental for making NCs of other structurally soft metal halides and, eventually, complex heterostructures.
3) Emitters with radiative rates exceeding decoherence rates are highly desirable for quantum light applications, as they enable coherent single-photon sources capable of producing indistinguishable photons.[41] LHP NCs have shown promising results, achieving photon indistinguishability up to 56%.[43] Building on these advancements, future research could unlock applications of LHP NCs as reliable and scalable quantum light sources in quantum computing[44] and quantum imaging.[45]
4) Despite the promising combination of properties, the potential of LHP NCs for photocatalysis remains largely underexplored. This limited focus on photocatalysis is understandable, given the demanding stability requirements for photocatalysts and the common belief that LHP NCs lack sufficient durability. However, recent advancements in refining the surface chemistry of these NCs present an exciting opportunity to realize their potential for photocatalytic applications through both energy transfer and direct photoredox catalysis. We anticipate that future studies will concentrate on organic transformations in mildly polar solvents. Energy transfer photocatalysis could benefit from the high absorption cross-section of LHP NCs combined with the long-lived triplet states of organic acceptor compounds.[46] The direct photoredox catalysis with LHP NCs could leverage the dynamic binding of ligands and surface lability to drive halogenation/dehalogenation of small organic molecules or other reactions for the substrates that readily adsorb on LHP surface.

Acknowledgements

We thank Dr. G. Rainò and S. Boehme for reading the manuscript. This publication was created as part of NCCR Catalysis (grant number 225147), a National Centre of Competence in Research funded by the Swiss National Science Foundation. This work was financially supported by the European Research Council through the European Union's Horizon 2020 programme (ERC Consolidator Grant SCALE-HALO, agreement no. 819740).

Received: November 14, 2024

[1] a) A. Kojima, K. Teshima, Y. Shirai, T. Miyasaka, *J. Am. Chem. Soc*. **2009**, *131*, 6050, https://doi.org/10.1021/ja809598r; b) M. M. Lee, J. Teuscher, T. Miyasaka, T. N. Murakami, H. J. Snaith, *Science* **2012**, *338*, 643, https://doi.org/doi:10.1126/science.1228604; c) J. Burschka, N. Pellet, S.-J. Moon, R. Humphry-Baker, P. Gao, M. K. Nazeeruddin, M. Grätzel, *Nature* **2013**, *499*, 316, https://doi.org/10.1038/nature12340.

[2] L. Protesescu, S. Yakunin, M. I. Bodnarchuk, F. Krieg, R. Caputo, C. H. Hendon, R. X. Yang, A. Walsh, M. V. Kovalenko, *Nano Lett*. **2015**, *15*, 3692, https://doi.org/10.1021/nl5048779.

[3] N. P. Gallop, D. R. Maslennikov, N. Mondal, K. P. Goetz, Z. Dai, A. M. Schankler, W. Sung, S. Nihonyanagi, T. Tahara, M. I. Bodnarchuk, M. V.

Kovalenko, Y. Vaynzof, A. M. Rappe, A. A. Bakulin, *Nat. Mater*. **2024**, *23*, 88, https://doi.org/10.1038/s41563-023-01723-w.
[4] J. De Roo, M. Ibáñez, P. Geiregat, G. Nedelcu, W. Walravens, J. Maes, J. C. Martins, I. Van Driessche, M. V. Koyalenko, Z. Hens, *ACS Nano* **2016**, *10*, 2071, https://doi.org/10.1021/acsnano.5b06295.
[5] D. N. Dirin, L. Protesescu, D. Trummer, I. V. Kochetygov, S. Yakunin, F. Krumeich, N. P. Stadie, M. V. Kovalenko, *Nano Lett*. **2016**, *16*, 5866, https://doi.org/10.1021/acs.nanolett.6b02688.
[6] G. Nedelcu, L. Protesescu, S. Yakunin, M. I. Bodnarchuk, M. J. Grotevent, M. V. Kovalenko, *Nano Lett*. **2015**, *15*, 5635, https://doi.org/10.1021/acs.nanolett.5b02404.
[7] a) L. Protesescu, S. Yakunin, M. I. Bodnarchuk, F. Bertolotti, N. Masciocchi, A. Guagliardi, M. V. Kovalenko, *J. Am. Chem. Soc*. **2016**, *138*, 14202, https://doi.org/10.1021/jacs.6b08900; b) O. Vybornyi, S. Yakunin, M. V. Kovalenko, *Nanoscale* **2016**, *8*, 6278, https://doi.org/10.1039/c5nr06890h; c) L. Protesescu, S. Yakunin, S. Kumar, J. Bär, F. Bertolotti, N. Masciocchi, A. Guagliardi, M. Grotevent, I. Shorubalko, M. I. Bodnarchuk, C. J. Shih, M. V. Kovalenko, *ACS Nano* **2017**, *11*, 3119, https://doi.org/10.1021/acsnano.7b00116; d) M. I. Bodnarchuk, L. G. Feld, C. Zhu, S. C. Boehme, F. Bertolotti, J. Avaro, M. Aebli, S. H. Mir, N. Masciocchi, R. Erni, S. Chakraborty, A. Guagliardi, G. Rainò, M. V. Kovalenko, *ACS Nano* **2024**, *18*, 5684, https://doi.org/10.1021/acsnano.3c11579.
[8] N. Yazdani, M. I. Bodnarchuk, F. Bertolotti, N. Masciocchi, I. Fureraj, B. Guzelturk, B. L. Cotts, M. Zajac, G. Rainò, M. Jansen, S. C. Boehme, M. Yarema, M.-F. Lin, M. Kozina, A. Reid, X. Shen, S. Weathersby, X. Wang, E. Vauthey, A. Guagliardi, M. V. Kovalenko, V. Wood, A. M. Lindenberg, *Nat. Phys*. **2024**, *20*, 47, https://doi.org/10.1038/s41567-023-02253-7.
[9] a) I. Lignos, S. Stavrakis, G. Nedelcu, L. Protesescu, A. J. deMello, M. V. Kovalenko, *Nano Lett*. **2016**, *16*, 1869, https://doi.org/10.1021/acs.nanolett.5b04981; b) R. M. Maceiczyk, K. Dümbgen, I. Lignos, L. Protesescu, M. V. Kovalenko, A. J. deMello, *Chem. Mater*. **2017**, *29*, 8433, https://doi.org/10.1021/acs.chemmater.7b02998.
[10] D. N. Dirin, B. M. Benin, S. Yakunin, F. Krumeich, G. Raino, R. Frison, M. V. Kovalenko, *ACS Nano* **2019**, *13*, 11642, https://doi.org/10.1021/acsnano.9b05481.
[11] L. Protesescu, S. Yakunin, O. Nazarenko, D. N. Dirin, M. V. Kovalenko, *ACS Appl. Nano Mater*. **2018**, *1*, 1300, https://doi.org/10.1021/acsanm.8b00038.
[12] Q. A. Akkerman, T. P. T. Nguyen, S. C. Boehme, F. Montanarella, D. N. Dirin, P. Wechsler, F. Beiglböck, G. Rainò, R. Erni, C. Katan, J. Even, M. V. Kovalenko, *Science* **2022**, *377*, 1406, https://doi.org/10.1126/science.abq3616.
[13] V. Morad, A. Stelmakh, M. Svyrydenko, L. G. Feld, S. C. Boehme, M. Aebli, J. Affolter, C. J. Kaul, N. J. Schrenker, S. Bals, Y. Sahin, D. N. Dirin, I. Cherniukh, G. Raino, A. Baumketner, M. V. Kovalenko, *Nature* **2024**, *626*, https://doi.org/10.1038/s41586-023-06932-6.
[14] M. I. Bodnarchuk, S. C. Boehme, S. ten Brinck, C. Bernasconi, Y. Shynkarenko, F. Krieg, R. Widmer, B. Aeschlimann, D. Günther, M. V. Kovalenko, I. Infante, *ACS Energy Lett*. **2019**, *4*, 63, https://doi.org/10.1021/acsenergylett.8b01669.
[15] F. Krieg, P. C. Sercel, M. Burian, H. Andrusiv, M. I. Bodnarchuk, T. Stöferle, R. F. Mahrt, D. Naumenko, H. Amenitsch, G. Rainò, M. V. Kovalenko, *ACS Cent. Sci*. **2021**, *7*, 135, https://doi.org/10.1021/acscentsci.0c01153.
[16] E. Scharf, F. Krieg, O. Elimelech, M. Oded, A. Levi, D. N. Dirin, M. V. Kovalenko, U. Banin, *Nano Lett*. **2022**, *22*, 4340, https://doi.org/10.1021/acs.nanolett.2c00611.
[17] D. Sarkar, A. Stelmakh, A. Karmakar, M. Aebli, F. Krieg, A. Bhattacharya, S. Pawsey, M. V. Kovalenko, V. K. Michaelis, *ACS Nano* **2024**, *18*, 21894, https://doi.org/10.1021/acsnano.4c02057.
[18] D. Guggisberg, S. Yakunin, C. Neff, M. Aebli, D. Günther, M. V. Kovalenko, D. N. Dirin, *Chem. Mater*. **2023**, *35*, 2827, https://doi.org/10.1021/acs.chemmater.2c03562.
[19] P. Tamarat, E. Prin, Y. Berezovska, A. Moskalenko, T. P. T. Nguyen, C. H. Xia, L. Hou, J. B. Trebbia, M. Zacharias, L. Pedesseau, C. Katan, M. I. Bodnarchuk, M. V. Kovalenko, J. Even, B. Lounis, *Nat. Commun*. **2023**, *14*, https://doi.org/10.1038/s41467-023-35842-4.
[20] A. Stelmakh, M. Aebli, A. Baumketner, M. V. Kovalenko, *Chem. Mater*. **2021**, *33*, 5962, https://doi.org/10.1021/acs.chemmater.1c01081.
[21] Y. Shynkarenko, M. I. Bodnarchuk, C. Bernasconi, Y. Berezovska, V. Verteletskyi, S. T. Ochsenbein, M. V. Kovalenko, *ACS Energy Lett*. **2019**, *4*, 2703, https://doi.org/10.1021/acsenergylett.9b01915.
[22] S. T. Ochsenbein, F. Krieg, Y. Shynkarenko, G. Rainò, M. V. Kovalenko, *ACS Appl. Mater. Interfaces* **2019**, *11*, 21655, https://doi.org/10.1021/acsami.9b02472.
[23] F. Krieg, S. T. Ochsenbein, S. Yakunin, S. ten Brinck, P. Aellen, A. Suess, B. Clerc, D. Guggisberg, O. Nazarenko, Y. Shynkarenko, S. Kumar, C. J. Shih, I. Infante, M. V. Kovalenko, *ACS Energy Lett*. **2018**, *3*, 641, https://doi.org/10.1021/acsenergylett.8b00035.
[24] F. Krieg, Q. K. Ong, M. Burian, G. Rainò, D. Naumenko, H. Amenitsch, A. Suess, M. J. Grotevent, F. Krumeich, M. I. Bodnarchuk, I. Shorubalko, F. Stellacci, M. V. Kovalenko, *J. Am. Chem. Soc*. **2019**, *141*, 19839, https://doi.org/10.1021/jacs.9b09969.
[25] I. Cherniukh, G. Rainò, T. Stöferle, M. Burian, A. Travesset, D. Naumenko, H. Amenitsch, R. Erni, R. F. Mahrt, M. I. Bodnarchuk, M. V. Kovalenko, *Nature* **2021**, *593*, 535, https://doi.org/10.1038/s41586-021-03492-5.
[26] G. Rainò, M. A. Becker, M. I. Bodnarchuk, R. F. Mahrt, M. V. Kovalenko, T. Stöferle, *Nature* **2018**, *563*, 671, https://doi.org/10.1038/s41586-018-0683-0.
[27] I. Cherniukh, T. V. Sekh, G. Rainò, O. J. Ashton, M. Burian, A. Travesset, M. Athanasiou, A. Manoli, R. A. John, M. Svyrydenko, V. Morad, Y. Shynkarenko, F. Montanarella, D. Naumenko, H. Amenitsch, G. Itskos, R. F. Mahrt, T. Stöferle, R. Erni, M. V. Kovalenko, M. I. Bodnarchuk, *ACS Nano* **2022**, *16*, 7210, https://doi.org/10.1021/acsnano.1c10702.
[28] I. Cherniukh, G. Rainò, T. V. Sekh, C. L. Zhu, Y. Shynkarenko, R. A. John, E. Kobiyama, R. F. Mahrt, T. Stöferle, R. Erni, M. V. Kovalenko, M. I. Bodnarchuk, *ACS Nano* **2021**, *15*, 16488, https://doi.org/10.1021/acsnano.1c06047.
[29] T. V. Sekh, I. Cherniukh, E. Kobiyama, T. J. Sheehan, A. Manoli, C. Zhu, M. Athanasiou, M. Sergides, O. Ortikova, M. D. Rossell, F. Bertolotti, A. Guagliardi, N. Masciocchi, R. Erni, A. Othonos, G. Itskos, W. A. Tisdale, T. Stöferle, G. Rainò, M. I. Bodnarchuk, M. V. Kovalenko, *ACS Nano* **2024**, *18*, 8423, https://doi.org/10.1021/acsnano.3c13062.
[30] J. Nette, F. Montanarella, C. L. Zhu, T. V. Sekh, S. C. Boehme, M. I. Bodnarchuk, G. Raino, P. D. Howes, M. V. Kovalenko, A. J. deMello, *Chem. Commun*. **2023**, *59*, 3554, https://doi.org/10.1039/d3cc00093a.
[31] a) H. Utzat, K. E. Shulenberger, O. B. Achorn, M. Nasilowski, T. S. Sinclair, M. G. Bawendi, *Nano Lett*. **2017**, *17*, 6838, https://doi.org/10.1021/acs.nanolett.7b03120; b) G. Rainò, N. Yazdani, S. C. Boehme, M. Kober-Czerny, C. L. Zhu, F. Krieg, M. D. Rossell, R. Erni, V. Wood, I. Infante, M. V. Kovalenko, *Nat. Commun*. **2022**, *13*, https://doi.org/10.1038/s41467-022-30016-0.
[32] M. V. Kovalenko, L. Protesescu, M. I. Bodnarchuk, *Science* **2017**, *358*, 745, https://doi.org/doi:10.1126/science.aam7093.
[33] Avafilm for LCD Backlights, https://avantama.com/markets/cadmium-free-quantum-dot-display/.
[34] N. A. Luechinger, *SID Symp. Dig. Tech. Pap*. **2020**, *51*, 1178, https://doi.org/https://doi.org/10.1002/sdtp.14088.
[35] Avapix for OLED & uLED Displays, https://avantama.com/markets/solution-processed-oled/.
[36] N. A. Luechinger, M. Oszajca, S. Loher, *SID Symp. Dig. Tech. Pap*. **2018**, *49*, 522, https://doi.org/https://doi.org/10.1002/sdtp.12451.
[37] H. Jiang, J. Lin, 'Micro LEDs', Academic Press, Cambridge, MA, **2021**.
[38] Display Week 2023 Highlights, https://doi.org/10.1002/msid.0050040.
[39] J. Shamsi, G. Rainò, M. V. Kovalenko, S. D. Stranks, *Nat. Nanotechnol*. **2021**, *16*, 1164, https://doi.org/10.1038/s41565-021-01005-z.
[40] M. A. Becker, R. Vaxenburg, G. Nedelcu, P. C. Sercel, A. Shabaev, M. J. Mehl, J. G. Michopoulos, S. G. Lambrakos, N. Bernstein, J. L. Lyons, T. Stöferle, R. F. Mahrt, M. V. Kovalenko, D. J. Norris, G. Rainò, A. L. Efros, *Nature* **2018**, *553*, 189, https://doi.org/10.1038/nature25147.
[41] C. L. Zhu, S. C. Boehme, L. G. Feld, A. Moskalenko, D. N. Dirin, R. F. Mahrt, T. Stöferle, M. I. Bodnarchuk, A. L. Efros, P. C. Sercel, M. V. Kovalenko, G. Rainò, *Nature* **2024**, *626*, 535, https://doi.org/10.1038/s41586-023-07001-8.
[42] a) C. Zhu, L. G. Feld, M. Svyrydenko, I. Cherniukh, D. N. Dirin, M. I. Bodnarchuk, V. Wood, N. Yazdani, S. C. Boehme, M. V. Kovalenko, G. Rainò, *Adv. Opt. Mater*. **2024**, *12*, 2301534, https://doi.org/https://doi.org/10.1002/adom.202301534; b) H. Utzat, W. W. Sun, A. E. K. Kaplan, F. Krieg, M. Ginterseder, B. Spokoyny, N. D. Klein, K. E. Shulenberger, C. F. Perkinson, M. V. Kovalenko, M. G. Bawendi, *Science* **2019**, *363*, 1068, https://doi.org/10.1126/science.aau7392.
[43] A. E. K. Kaplan, C. J. Krajewska, A. H. Proppe, W. Sun, T. Sverko, D. B. Berkinsky, H. Utzat, M. G. Bawendi, *Nat. Photonics* **2023**, *17*, 775, https://doi.org/10.1038/s41566-023-01225-w.
[44] C. R. Kagan, L. C. Bassett, C. B. Murray, S. M. Thompson, *Chem. Rev*. **2021**, *121*, 3186, https://doi.org/10.1021/acs.chemrev.0c00831.
[45] H. Defienne, W. P. Bowen, M. Chekhova, G. B. Lemos, D. Oron, S. Ramelow, N. Treps, D. Faccio, *Nat. Photonics* **2024**, *18*, 1024, https://doi.org/10.1038/s41566-024-01516-w.
[46] L. G. Feld, S. C. Boehme, V. Morad, Y. Sahin, C. J. Kaul, D. N. Dirin, G. Rainò, M. V. Kovalenko, *ACS Nano* **2024**, *18*, 9997, https://doi.org/10.1021/acsnano.3c11359.

License and Terms

The definitive version of this article is the electronic one that can be found at https://doi.org/10.2533/chimia.2024.862